Journal of Ecological Engineering Design jeed.pubpub.org

Research Case Study

Stream Restoration that Allows for Self-Adjustment Can Increase Channel-Floodplain Connectivity

Nicholas D. Christensen[1,2], Elizabeth M. Prior[1], Jonathan A. Czuba[1], W. Cully Hession[1]

[1]Department of Biological Systems Engineering, Virginia Tech, Blacksburg, Virginia, 24061, USA

[2]Now at the Department of Civil and Environmental Engineering, Colorado State University, Fort Collins, Colorado, 80523, USA

Correspondence
Nicholas D. Christensen
Department of Civil and Environmental Engineering
Colorado State University
Fort Collins, CO 80523, USA
Email: ndchris9@colostate.edu

Received
February 24, 2023
Accepted
October 15, 2023
Published
February 14, 2024

Editors
Marc Beutel,
Co-Editor in Chief
Anand Jayakaran,
Associate Editor

Streams are often "restored" to reduce sediment loading using one or a combination of practices such as livestock exclusion, riparian plantings, and/or bank reshaping and stabilization. Direct comparisons of how these methods affect stream processes, including channel-floodplain connectivity, over time are essential to informing restoration design. (Channel-floodplain connectivity is the ability of a stream to exchange water, sediment, and nutrients with its floodplain at high flows.) To investigate the impact these stream restoration practices have had on channel-floodplain connectivity, we developed a 2-D HEC-RAS hydraulic model for 3 restoration treatments along an urban and agriculturally impacted stream in southwest Virginia, United States. All 3 treatments excluded cattle in 2009. The farthest upstream treatment, Treatment 1, had no other intervention while the other two, Treatments 2 and 3, were regraded and stabilized, then replanted with native species (completed May 2010). The overhanging banks of Treatment 2 were regraded to a slope of 3:1, while those of Treatment 3 had a flat inset floodplain cut into the bank before sloping the banks at 3:1. During the 11-year monitoring timeline, prior work showed the streambanks in Treatment 1 migrated through both outer bank erosion and inner bank deposition with the autogenic creation of inset floodplains, while Treatments 2 and 3 had minimal bank adjustment. The adjusted geometry of Treatment 1 provided higher floodplain volume, channel-floodplain exchange flows, and flow moving across the floodplain than Treatments 2 and 3. Treatment 3 showed some metrics of higher connectivity than Treatment 2, but there was not uniform agreement between metrics. While the hydraulic analysis indicates a higher channel-floodplain connectivity in Treatment 1, active management of Treatments 2 and 3 has reduced the bank erosion rate and accelerated the riparian forest regrowth, providing other benefits including increased shading, wood supply, and vegetation diversity.

Keywords Bank stabilization; Cattle exclusion; Channel evolution; Ecohydraulics; Floodplain building

Christensen ND, Prior EM, Czuba JA, Hession WC. 2024. Stream Restoration that Allows for Self-Adjustment Can Increase Channel-Floodplain Connectivity. Journal of Ecological Engineering Design. https://doi.org/10.21428/f69f093e.e8ffa1a3

Treatment 1

Treatment 2

Treatment 3

Project photographs Treatment 1, photographed April 2022: Excluded cattle only. Treatment 2, photographed April 2022: Banks were regraded to a 3:1 slope, stabilized, and replanted with native species; also excluded cattle. Treatment 3, photographed April 2018: Inset floodplain was cut into the bank; the banks were then regraded to a 3:1 slope, stabilized, and replanted with native species; also excluded cattle. Photographs from 2010 and before are available in Wynn-Thompson et al. (2010).

1. Introduction

The ability of a stream to exchange water, sediment, and nutrients with its floodplain at high flows is referred to as channel-floodplain connectivity (Czuba et al. 2019). Channel-floodplain connectivity facilitates several important stream processes including vertical floodplain building, peak flow attenuation, and geochemical cycling (Lane 2017; McMillan and Noe 2017). Maintaining channel-floodplain connection is essential in river management as it is a major driver of hydraulics, morphology, sediment dynamics, and habitat diversity (Harman et al. 2012; Byrne et al. 2019). The channel-floodplain connectivity of a system has been quantified using multiple metrics rooted in hydraulic modeling. Perhaps the most basic form of quantification comes from looking at the flood extents and floodplain water depth (Hammersmark et al. 2008; Czuba et al. 2019; Rajib et al. 2021). This approach is expanded upon by looking specifically at exchanges of mass and momentum between a channel and its floodplain (Byrne et al. 2019; Czuba et al. 2019). Examining exchanges of mass and momentum allows for insight into biogeochemical processes and flood propagation. Researchers have explored channel-floodplain interactions with a channel-length-normalized flux of water to allow for comparison of the degree of connectivity between systems (Byrne et al. 2019; Czuba et al. 2019). By comparing the degree of channel-floodplain connectivity of river systems, we can also determine the relative differences in floodplain services between systems (Hammersmark et al. 2008; McMillan and Noe 2017).

A channel and floodplain with high connectivity can attenuate peak flows, deposit sediment, increase nutrient cycling, and promote higher biodiversity (Baldwin and Mitchell 2000; Clawson et al. 2001; Brierley and Fryirs 2005; Hammersmark et al. 2008; Bellmore and Baxter 2014; Göthe et al. 2016; Palmer and Ruhi 2019; Karpack et al. 2020). While this connectivity provides desirable services, the floodplain is often disconnected by anthropogenic alterations (Simon and Hupp 1987; Bernhardt et al. 2005; Brierley and Fryirs 2005; Gergel et al. 2005). Among these alterations are channelization, artificial levee building, wetland drainage, and damming (Brierley and Fryirs 2005). Of particular importance in headwater streams is the practice of channelization, which often involves straightening, widening, and deepening to increase the stream's capacity to transport and contain flow in the channel (Bernhardt et al. 2005; Simon et al. 2011). The altered channel quickly moves water through the landscape without interacting with the floodplain. This reduction in channel-floodplain connectivity has had unforeseen consequences, including significant damage to natural stream structure, stream ecosystems, and a lack of flood dissipation leading to larger floods downstream (McMillan and Noe 2017; Knox et al. 2022).

Highlight
2D modeling of a stream restoration project indicates the highest surface water channel-floodplain connection is in the section of stream without bank regrading or stabilization.

Stream restoration is often used as a tool to revert channelized streams to a state that has higher channel-floodplain connectivity (Brookes and Shields 1996; Bernhardt et al. 2005; Hammersmark et al. 2008; Simon et al. 2011). These changes often are aimed at enhancing aquatic habitat, dissipating floodflow energy, decreasing peak flows, and reducing bank erosion (Bernhardt et al. 2005; Wynn-Thompson et al. 2010; McMillan and Noe 2017). Restoration practitioners often alter river corridors with heavy machinery, herein referred to as active restoration. Active restoration aims to either stabilize the current river channel or accelerate the evolution of the channel into a dynamic equilibrium that would theoretically be reached given enough time for channel adjustment (Simon and Hupp 1987; Levell and Chang 2008). Clear cutting and soil compaction, which are unavoidable, are unwanted side effects of making channel adjustments (Bernhardt et al. 2005; Bernhardt and Palmer 2011; Laub et al. 2013). For the past several years, there has been a call to move away from changing the form of rivers through active regrading projects toward efforts to influence river processes through less intensive management activities (Beechie et al. 2010; Bernhardt and Palmer 2011; Wohl et al. 2015). Passive forms of restoration, including cattle exclusion (allowing for bank migration) and planting woody riparian zones, have also been implemented to influence channel form and uplift local ecosystems (Trimble 1994; Brookes and Shields 1996; Bernhardt and Palmer 2011; Chardon et al. 2022).

How we define the success of a restoration project is an active field of study. Geomorphic stability, hydraulic performance, and biological integrity are aspects of streams that restoration practitioners intend to change (Bernhardt and Palmer 2011; McMillan and Noe 2017). Prior efforts to monitor restored sites have been criticized for having short study times and limited parameters of investigation (Wohl et al. 2015; Rubin et al. 2017). Monitoring for geomorphic stability and biological integrity is fairly standard and relies mostly on repeated surveys of stream geometry, woody vegetation, and benthic macroinvertebrate populations (Bernhardt et al. 2005). Quantifying channel-floodplain reconnection is less standardized, but has been published in some case studies (Hammersmark et al. 2008; Bernhardt and Palmer 2011; McMillan and Noe 2017). Previous studies have modeled the pre- and post-restoration forms of a fully regraded stream and found increased floodplain inundation (Hammersmark et al. 2008; Sholtes 2009). These studies differed from our study reach in that they focused on streams that had been completely redesigned using large rock structures for stabilization, whereas our system was only adjusted in cross section with no grade stabilization structures. While this work indicates that the fully regraded and stabilized channels can provide higher channel-floodplain connectivity immediately after construction, the long-term (10+ years) channel-floodplain connectivity was not explored, nor were comparisons made with other passively adjusting streams.

The objective of this case study was to present the first-known direct comparison of channel-floodplain connectivity between actively and passively restored treatments of the same stream. Additionally, we examined the influence of time on the hydraulic function of a restored stream with data 11 years after restoration. Understanding the hydraulic differences between actively and passively restored reaches is of the utmost importance when practitioners are highly incentivized to implement streambank regrading projects (Wohl et al. 2015). We aim to fill this gap in our understanding by using direct comparison of the hydraulic characteristics in a stream with a mix of common regrading treatments and a naturally adjusting stream reach. In doing so, we aim to inform the discussion on design and regulation of restored streams to promote more effective stream restoration for achieving the goal of floodplain reconnection.

2. Case Study Site

The study site is a reach of Stroubles Creek in Blacksburg, Virginia, United States, called the Stream Research, Education and Management (StREAM) Lab (Fig. 1). The stream is in the Valley and Ridge physiographic province of Virginia. The contributing watershed is highly urbanized with 81% urban land cover (USGS 2019). The studied reach of stream has a 1,530 ha drainage area, bankfull width of 9.4 m, 0.22% slope, and sinuosity of 1.1. The hillslope has cultivated crops on the southeast side of the stream and a cow pasture on the northwest. Prior to the stream restoration in 2010, the entire stream and floodplain were in cow pasture. The riparian grazing limited

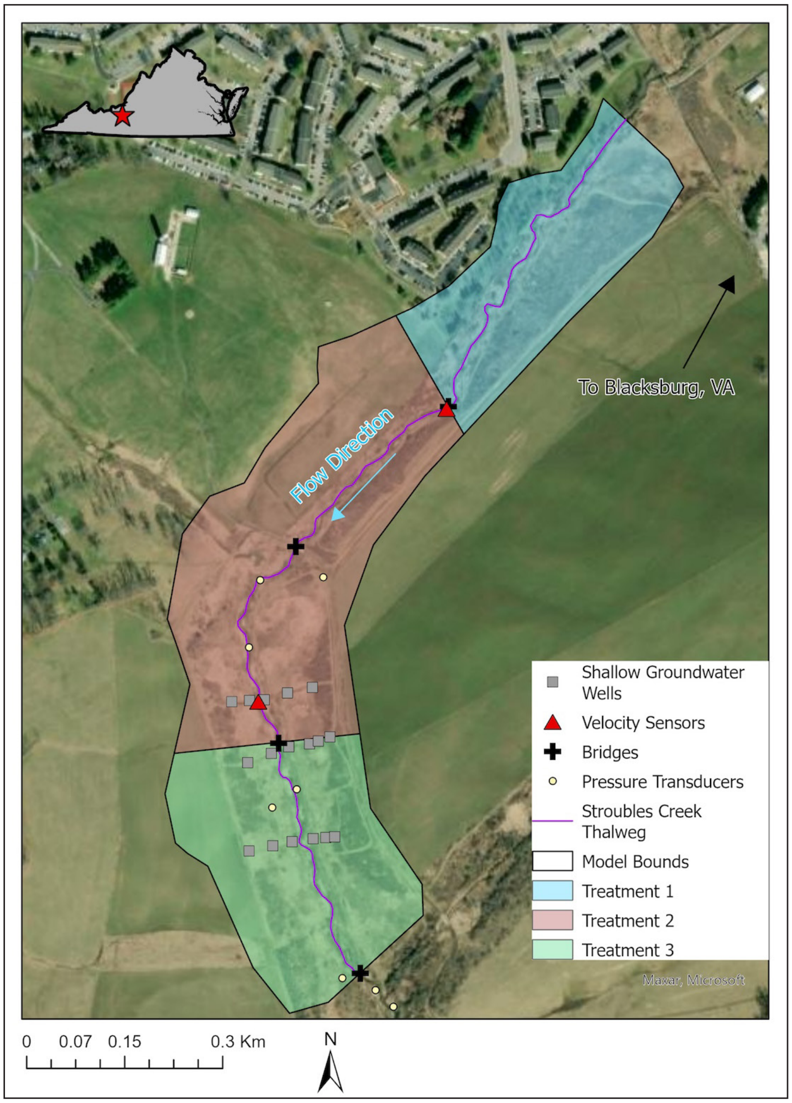

Fig. 1 Study area of Stroubles Creek, called the Stream Research, Education and Management (StREAM) Lab, in Blacksburg, Virginia, United States, with the treatments of restoration and locations of relevant instrumentation indicated. ArcGIS Pro imagery from 2020. Sources: Maxar, Microsoft.

the vegetation to short grasses and led to highly unstable banks. The estimated bankfull, 2-year, and 10-year recurrence interval flows as predicted by the Virginia Tech/Penn State Urban Hydrology Model are 6.4 m^3/s, 12.5 m^3/s, and 40 m^3/s, respectively (Wynn-Thompson et al. 2010).

Stroubles Creek was first designated as impaired for aquatic life on the 303(d) list of impaired waters in 1996 due to an excess of fine sediment loading (USEPA 2020). While turbidity levels have declined since then, this designation still stands as of the writing of this manuscript. The studied stream restoration project was implemented in 2010 with a goal to reduce sediment loading from bank erosion (Wynn-Thompson et al. 2010). While the restoration engineers suspected the stream had been channelized, they found the pre-restoration entrenchment ratio of 6.1 acceptable (Wynn-Thompson et al. 2010). Their restoration did not have the stated goal of influencing channel-floodplain connectivity that we focus on primarily as part of this study. They utilized 3 restoration techniques in 3 separate stream reaches referred to as Treatments 1, 2, and 3 with the treatment number increasing moving downstream, as shown in Fig. 1. Each of the restoration techniques used, including the regrading angle, bank stabilization, and replanting techniques, is a commonly implemented standard in stream restorations across the United States (Anderson et al. 2007; Wynn-Thompson et al. 2010).

Treatment 1 (valley length 480 m) was passively restored by removing cattle using fencing. The 2 reaches downstream (Treatment 2: 510 m and Treatment 3: 300 m) also excluded cattle and were actively restored by regrading and stabilizing the vertical streambanks without in-stream construction (Fig. 2). After regrading, these actively restored treatments of the stream were stabilized with native vegetation and coir fiber matting. The banks of Treatment 2 were regraded from nearly vertical to a 3:1 slope. Treatment 3 had a 2-stage channel design (or inset floodplain) with a lower bench between 0.4 m – 0.5 m above the thalweg, then sloped 3:1 to an elevation of approximately 0.7 m – 0.8 m above the thalweg, which was then sloped to the upper floodplain elevation (Wynn-Thompson et al. 2010; Resop et al. 2014; Hendrix 2022).

Treatment 1 has the highest stream slope at 0.30% and the highest sinuosity at 1.15. Treatment 2 has a lower stream slope and sinuosity at 0.20% and 1.05, respectively. Treatment 3 has intermediate values between Treatments 1 and 2 with stream slope and sinuosity of 0.25% and 1.13, respectively. Regrading efforts were focused on changing cross-sectional geometry, meaning these differences in longitudinal and planform geometry are due to the pre-restoration conditions and post-restoration adjustment. For this study we delineated the

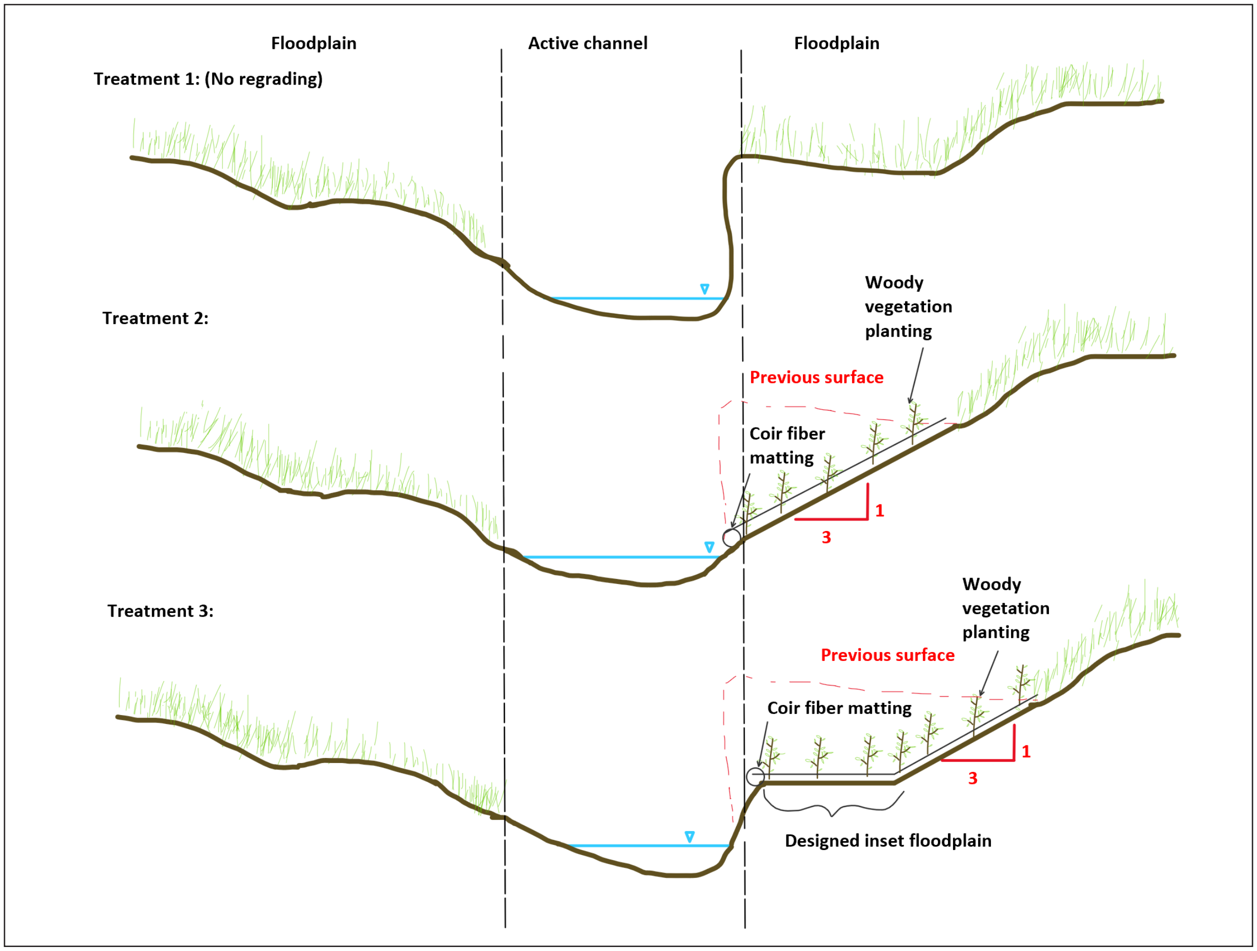

Fig. 2 Conceptual diagram of cross sections immediately after restoration treatments were applied (not to scale).

channel/floodplain boundary at the extent of the low flow channel, which was defined as the portion of channel without permanent vegetation (typically wet during low flow) and was always below any inset floodplains (Fig. 2). That is, the inset floodplain was considered part of the floodplain when we refer to the channel versus the floodplain in this study.

The StREAM Lab has been instrumented to collect hydrologic, water quality, and hydraulic data to characterize separate reaches of the stream. Stage has been measured with pressure transducers, for more than 10 years at 15-min increments, attached to the bridges at the interface of Treatments 1-2 and 2-3. Additionally, there are two in-situ SonTek-IQ Plus uplooking acoustic Doppler velocimeters (SonTek-IQ – a Xylem brand, San Diego, California, United States) in the channel that have been recording data since 2019, averaging velocities over a 2-min period and recording data every 5 min. A mowed path has been maintained within the floodplain to provide access to the stream and for equipment maintenance.

Dominant soils in the floodplain are McGary and Purdy soils, which are deep soils (~2 m to restrictive layer) characterized by high clay content and slightly poor drainage. The stream banks are composed of this cohesive soil and are well vegetated with grasses, shrubs, and trees. While there is more mature native vegetation in Treatments 2 and 3, the overall density of woody vegetation is highest in Treatments 1 and 3 (Hendrix 2022). There are some small outcroppings of bedrock in Treatment 1 that control grade, whereas the rest of the bed is composed of gravel and sand. The median particle size (D50) has been reported ranging from 11 mm – 29 mm (Abel et al. 2016). The banks contain significant fractions of clay, ~25% of which has shrink-swell properties causing mass wasting during these cycles (Wynn et al. 2008).

Previous research monitoring the channel evolution at the site has shown major adjustments in Treatment 1 since the restoration in 2010 (Hendrix 2022). Repeat cross sections during the last decade show that the cut banks of Treatment 1 have eroded ~1 m laterally. Opposite the cutting banks, an inset floodplain was formed through vertical accretion of 0.4 m of sediment. This accretion resulted in a floodplain that was on average 0.45 m above the channel thalweg. The benches of the inset floodplains observed in Treatment 1 were non-uniform, with some low-lying places forming small floodplain channels. The formation of new floodplain did not fully reconnect the stream with its historic floodplain, as there was still another 0.5 m between the inset floodplain and the main valley floor. These adjustments reduced the channel area in Treatments 1 and 2 and slightly increased the channel area in Treatment 3. Adjustments in Treatments 2 and 3 are generally less extreme than those observed in Treatment 1, which Hendrix (2022) attributed to the bank stabilization.

3. Materials and Methods

3.1 Model Development

We developed a 2-dimensional hydraulic model in the U.S. Army Corps of Engineers Hydrologic Engineering Center River Analysis System (HEC-RAS 2-D, version 5.0.7). The terrain we used in our hydraulic model was a Digital Elevation Model (DEM) derived from drone lidar data and surveyed bathymetry. We collected the lidar data with the same system as described in Prior et al. (2022), which included a Vapor35 drone (AeroVironment, Simi Valley, California, United States) equipped with a YellowScan Surveyor Core lidar system (Monfeerier-sur-Lez, France) and a GNSS-inertial Trimble APPLANIX APX-15 (Trimble, Richmond Hill, Ontario, Canada). We planned the flight using the wePilot1000 flight control system and the weGCS ground control system software (weControl SA, Courtelary, Switzerland) with the drone maintaining 30 m of altitude and scanning 20-m wide flight lines. The size of the site necessitated 2 flights, on 2021 November 17 and 2021 December 10. The data was corrected using a local CORS base station. The data was exported as LAS file format in NAD83 UTM zone 17N. The separate scanline files were then aligned using CloudCompare software (https://www.danielgm.net/cc/), where the drone lidar point cloud was aligned with the 2018 Virginia Geographic Information Network lidar point cloud (Virginia FEMA 2018) and surveyed points of the bridges. We aligned the point cloud using a minimum filter and iterative closest point methodology within CloudCompare (Prior et al. 2022). From this aligned point cloud, ground points were identified using the simple morphological filter (Pingel et al. 2013). Ground points were then passed through a natural neighbor interpolator using the "LAS Dataset to Raster" tool within ArcGIS Pro, version 2.9.2 (ESRI, Redlands, California, United States). This created a DEM raster at 0.1 m resolution.

We collected a bathymetric survey with a Trimble R10 GNSS System (Trimble, Sunnyvale, California, United States) from mid-November 2022 to December 2022. Cross sections were measured from top of bank to top of bank, measuring a minimum of 5 points: 2 points for the top of each bank, 2 for the toe of each bank, and one for the thalweg. Cross sections were spaced at approximately every 7 m (less than 2 low flow channel widths). A higher density of cross sections was measured in areas of rapid bathymetric change to best capture the geometry of the stream. We post-processed the GNSS points using the OPUS correction (OPUS 2023). All cross sections were plotted along their nearest upstream and downstream neighboring sections and visually inspected for quality control. We created an elevation model of the bathymetry using only points in the channel with ArcGIS Pro's function "Raster from topo" that interpolates between the measured data points in 2D space, creating a representation of the topography with 0.1 m cells. The lidar-based DEM and bathymetry were then mosaicked into one DEM using ArcGIS Pro's "Mosaic to new raster" with the preference for the bathymetric DEM where data overlapped. The final geometry was published by Hession et al. (2023).

There are 4 bridges within the boundary of the model domain. We modeled the bridges as only abutments with the deck omitted. During modeling we determined that the extent of the drone lidar was not sufficient to allow for simulation of the highest flows. To extend our model we used a 1 m DEM from USGS (USGS 2021) to extend the model geometry farther up the hillslope. Integration of this 1 m DEM with the existing 0.1 m DEM was completed in RAS-Mapper, as it allows for tools to create terrain files that have different cell spacing. Where data overlapped, the 0.1 m DEM was preferred.

The computational mesh created for the 2D flow simulation included 2 areas, with finer spacing in the main channel corridor (which includes any inset floodplains) and coarser spacing on the upper floodplain and adjacent hillslopes. The spacing was defined with refinement regions in HEC-RAS. Spacing for the inner region was set to 1 m with additional refinement occurring at the breaklines, which were set on the banks. Spacing was set as finely as possible while maintaining model stability with timesteps of 0.25 s for the largest modeled flows. The upper floodplain cell size was set to 2 m, again with the aim of minimizing mesh size while maintaining model stability. The upstream boundary condition was specified with a flow series and the downstream boundary condition was set as a normal depth assumption with an energy slope equal to the site average stream slope of 0.22%.

3.2 Model Calibration

Model calibration was completed by adjusting Manning's roughness values until the simulated rating curve matched the observed stage-discharge relationship measured by the main channel in situ velocity sensor at Bridge 2. Roughness was set in 3 different zones, the channel, floodplain, and mowed access path. Initial roughness values were set as 0.04, 0.50, and 0.04 for the channel, floodplain, and access path, respectively, based on a previous model created by Prior et al. (2021). Roughness values were assumed to be independent of flow depth over the range of modeled flows. Flows every 1 m^3/s from 2 m^3/s – 12 m^3/s were simulated in the model and steady state water-surface elevation (WSE) was recorded for each simulated flow. The difference between the model results and the best fit of the velocity sensor was quantified using a root mean square error (RMSE). The best fit developed for the in-channel velocity data was a piecewise function with a break at 4 m^3/s. Below 4 m^3/s, the data followed a linear trend while above it, the data followed a power function. Using the RMSE and visual inspections of the data, the roughness was iteratively adjusted to best agree with the velocity sensor within its 95% prediction interval.

3.3 Model Evaluation

After model calibration we simulated 4 observed peak flows of 5.4 m^3/s, 6.8 m^3/s, 7.2 m^3/s, and 10.3 m^3/s. We chose these flow events because flows less than 5 m^3/s did not inundate many of the pressure transducers on the floodplain, reducing the number of data points that could be compared to the modeled WSE. The peak of each event was run until the model reached steady state, at which time the WSE profile was extracted. We then compared the modeled WSE profile to all collected pressure transducer data from the observed peak. Not all pressure transducers were able to capture every event, so the number of observations for each peak varied depending on which pressure transducers were inundated and operational.

3.4 Model Simulations

After model calibration and evaluation, we simulated a final set of flows within the range of the calibration flows. The final model simulations ranged from 3 m^3/s – 12 m^3/s and were run until steady state was reached. Below 7 m^3/s, we recorded steady state values every 0.25 m^3/s. With larger flows we observed smaller changes in WSE, so we increased the flow step size to 0.5 m^3/s between 7 m^3/s – 10 m^3/s, and to 1 m^3/s between 10 m^3/s – 12 m^3/s, representing moderate floods with a recurrence interval ≥2 yrs. In all, at least one simulation was performed for each 5 mm interval of WSE measured at the in situ velocity sensor at Bridge 2. Steady-state conditions for each flow were output as rasters and text files, with hydraulic depth and 2D velocity at each cell center (Czuba et al. 2019). Steady-state conditions were exported as water depth rasters at each modeled peak flow event; the most insightful flows are shown as results.

3.5 Channel-Floodplain Connectivity Metric Calculations

Four metrics—normalized floodplain volume, fraction of flow moving within the floodplain, flux into the floodplain, and floodplain residence time—were chosen to explore the channel-floodplain dynamics of each treatment. The normalized floodplain volume represents the extent of floodplain activation (Hammersmark et al. 2008; Opperman et al. 2010) with the bias of reach length removed for comparison between sites. The fraction of flow moving though the floodplain represents the relief of flows that the floodplain provides, which is an essential service in preserving habitat for aquatic and riparian species (McKean and Tonina 2013; Amoros and Bornette 2002). The channel-floodplain exchange directly explores the degree of surface water connection (Czuba et al. 2019; Byrne et al. 2019). The exchange and residence time also have implications for sediment and nutrient cycling (Clawson et al. 2001; Gergel et al. 2005; Holmes et al. 1994). A more connected floodplain will have higher normalized volume, exchange rates, and flow within the floodplain. High connectivity may also lead to lower residence times as water moves between the channel and floodplain more readily.

We read the text file outputs of HEC-RAS into MATLAB (Version 2018b, MathWorks Inc., Natick, Massachusetts, United States) for further analysis using a script developed by Czuba et al. (2019). In MATLAB, we interpolated the depth and 2D velocity outputs into a regularly spaced grid. Floodplain volume (m^3) was calculated by multiplying the average depth (m) of all cells contained in the floodplain by the cell area (m^2). Average channel depth and velocity were taken by averaging the depth and velocity raster values contained in the channel polygon. These grids of velocity and depth were then multiplied by each other to create a grid of cell-specific discharge (m^2/s). Channel-floodplain exchange (m^3/s) was calculated following the approach of Czuba et al. (2019) by interpolating the cell-specific discharge (m^2/s) to points generated along each bank, calculating the component of this vector that is perpendicular to the bank, then multiplying by the spacing between the calculation points on the bank (m). The total flux (m^3/s) into the floodplain of each reach was calculated by summing the positive projected specific discharge (m^2/s) and

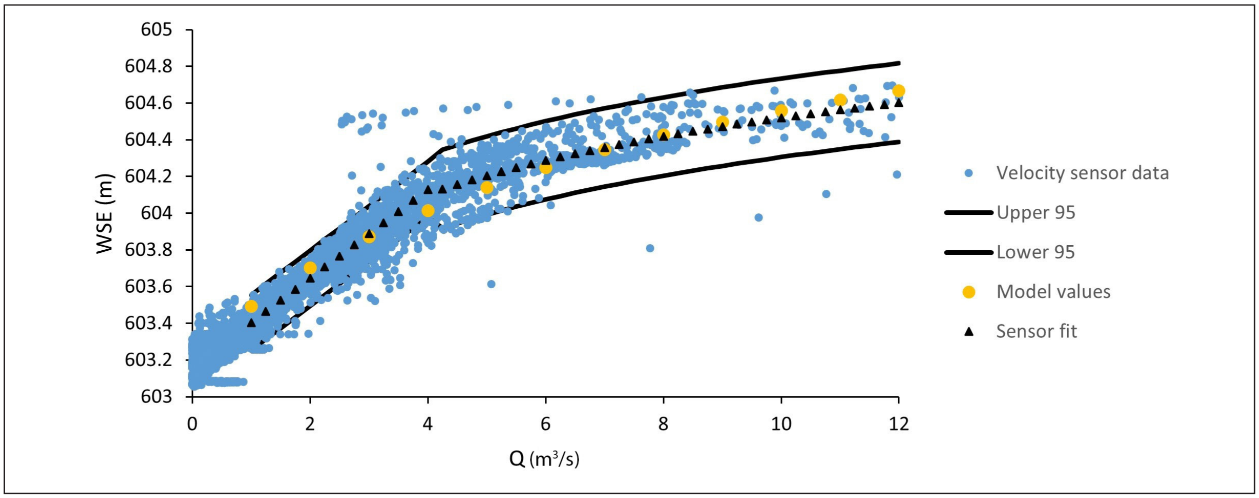

Fig. 3 Calibrated model results, simulated streamflow (Q) and water surface elevation (WSE) data compared to the observed data from the in situ velocity sensor at Bridge 2 along with the piecewise fit to the sensor data.

multiplying by the spacing (m). Average discharge per unit length (m^2/s) was then calculated by dividing the flux into the floodplain (m^3/s) by the reach length (m). Floodplain residence time (s) was calculated by dividing the volume of water in the floodplain (m^3) by the flux into the floodplain (m^3/s). Floodplain volume was normalized by dividing floodplain volume of each treatment by the volume in the channel in that treatment. We calculated the average flow within the floodplain by subtracting the channelized flow calculated at cross sections every 10 m from the total flow. We then calculated width statistics for these cross sections to explore differences in channel form.

4. Results

4.1 Model Calibration and Evaluation

Calibration to the observed streamflow (Q)-(WSE) relationship yielded best-fit roughness values of 0.05, 0.45 and 0.04 for the channel, floodplain, and access path, respectively. The fully calibrated model produced a RMSE of 5.6 cm with all modeled flows falling within the 95th prediction interval of the collected data (Fig. 3).

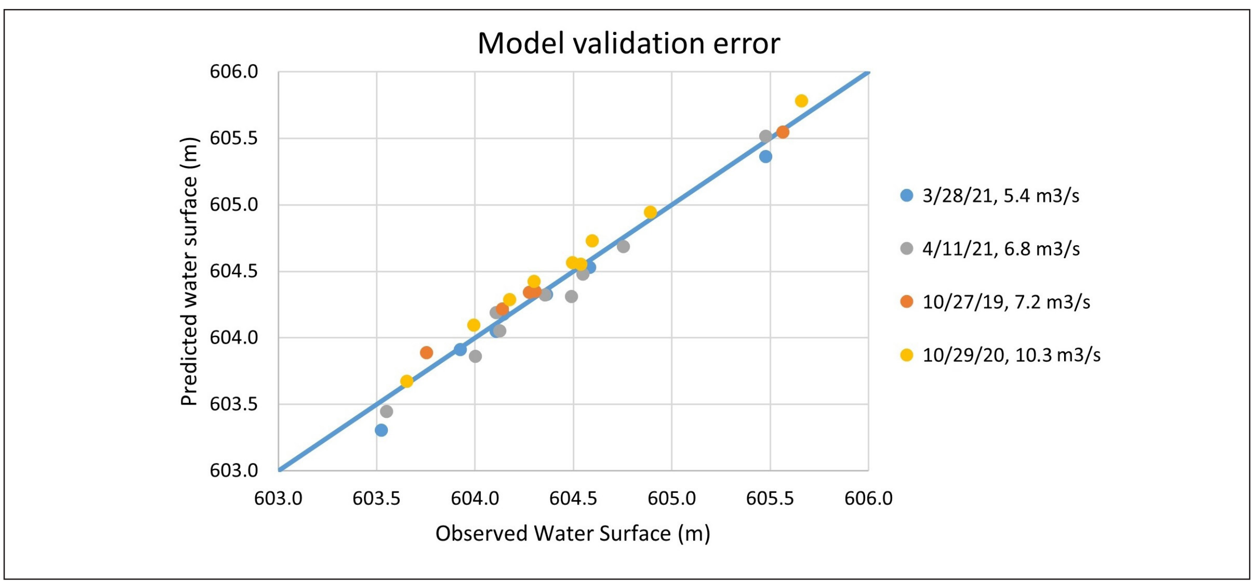

Fig. 4 Evaluation of model comparing the predicted water surface to the pressure transducer observations.

The 4 evaluation runs of observed peak flows had an RMSE of below 10 m^3/s (Fig. 4). These runs showed less accuracy than the calibration runs, likely because of spatial nonuniformity in roughness, which was spatially constant in the model over the 3 zones. All 4 evaluation runs showed acceptable error with the RMSE of each run below values found in a similar 2-D HEC-RAS model of the same reach with more complex characterizations of roughness (Prior et al. 2021).

4.2 Channel-Floodplain Connection

Model simulations revealed that the floodplain channels of Treatment 1 are activated during flows as low as 3 m^3/s (Fig. 5B and Fig. 5C). While some small floodplain channels close to the main channel can be seen in Treatments 2 and 3, they are less numerous and widespread than in Treatment 1 (Fig. 5D and Fig. 5E). These floodplain channels usually spanned one meander length and brought water out onto the floodplain before quickly returning to the main channel.

Flow in Treatment 1 was on average deeper and slower moving than flow in Treatments 2 and 3 (Fig. 6A and Fig. 6B). The velocities in Treatment 3 are nearly the same as observed in Treatment 2 (Fig. 6B). Though the median channel width of Treatment 1 is smaller, moderate floods (≤ 6 m^3/s) inundate a larger width, likely due to the low-lying inset floodplain in Treatment 1 (Fig. 6C and Fig. 6D). During large floods the entire valley is inundated and the wetted widths of Treatments 2 and 3 overtake that of Treatment 1. This points to a wider main valley in Treatments 2 and 3 (Figure 6D).

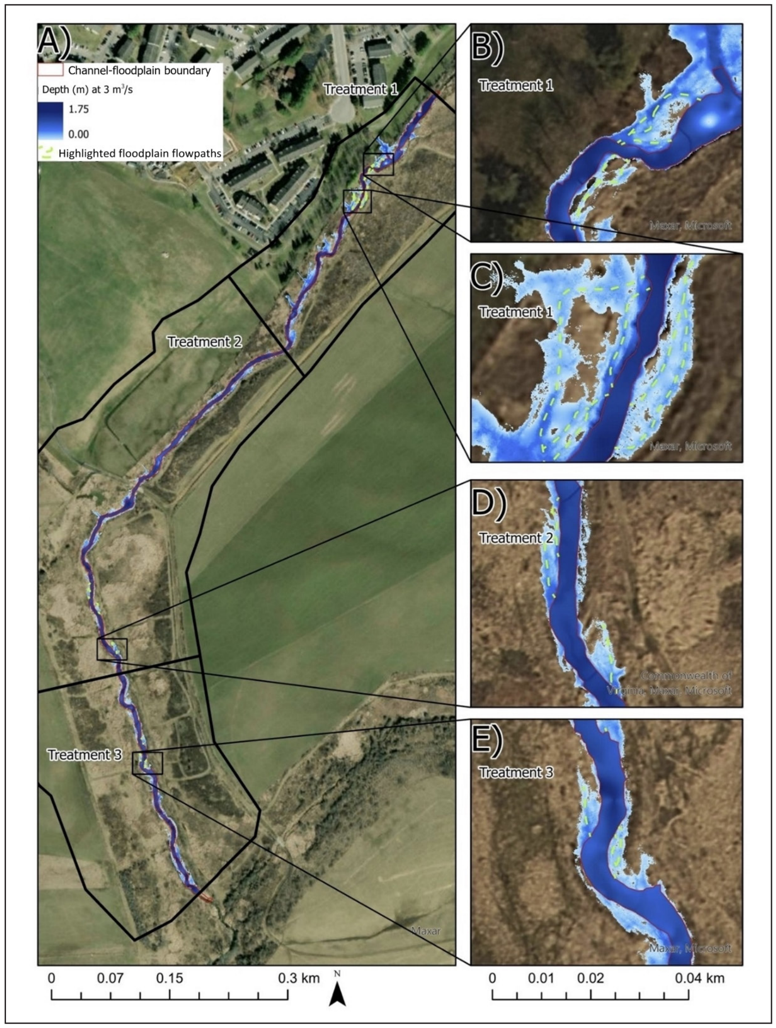

Fig. 5 Simulated depths at 3 m^3/s. Key areas are highlighted to show the differences in flow paths within the floodplain for each treatment. ArcGIS Pro imagery from 2020. Sources: Esri, Maxar, Earthstar Geographics, and the GIS User Community.

The calculated metrics for channel-floodplain connectivity (normalized floodplain volume, fraction of flow in the floodplain, and channel-floodplain exchange) indicate that Treatment 1 has the highest channel floodplain connectivity, followed closely by Treatment 3, while Treatment 2 has consistently low connectivity (Fig. 7). The normalized volume of water in the floodplain (floodplain volume/channel volume) was higher in Treatment 1 than in either regraded treatment for lower magnitude flows (Fig. 7A). For flows >7 m^3/s, the floodplain volumes for Treatment 1 and 3 were very similar, with Treatment 3 having up to 4% higher normalized floodplain volume than Treatment 1. At all flows, Treatment 2 had the lowest normalized floodplain volume. Treatments 1 and 3 had similar fractions of their flow in the floodplain, with Treatment 2 consistently having 3% of its flow contained in the main channel compared with Treatments 1 and 3 (Fig. 7B). Treatment 1 had the highest water exchange between the channel and its floodplain at all modeled flows (Fig. 7C). Channel-floodplain exchange increased with increasing discharge, as did the differences between the sites. Treatment 1 had channel-floodplain exchange up to 84% higher than Treatment 2 and 209% higher than Treatment 3. Residence time in the floodplain was highest in Treatment 1 during moderate floods, but during high flows, both active treatments had higher residence times (Fig. 7D). This may have been due to the higher density of floodplain channels in Treatment 1 or the higher valley slope of Treatment 1.

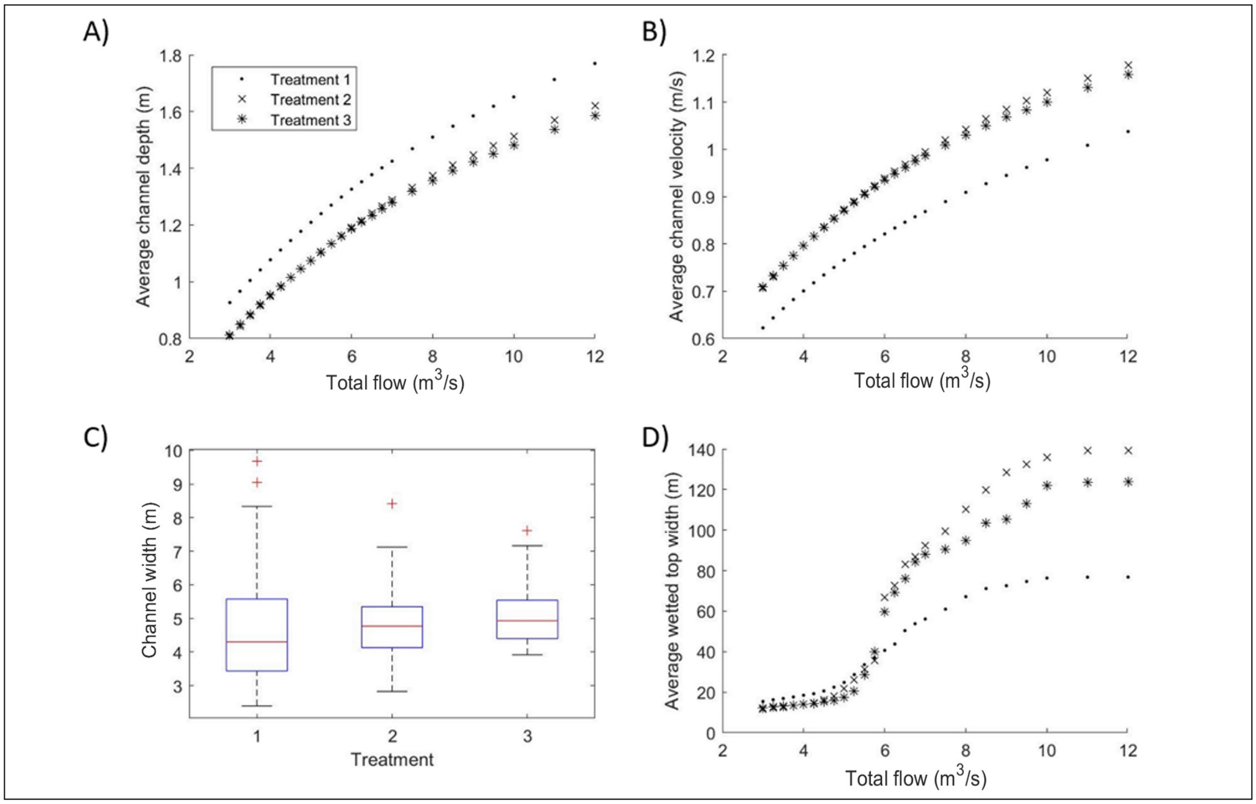

Fig. 6 Flow and channel characteristics of each treatment in 2021 (11 yrs after restoration) over the range of modeled flows including: A) average depth within the channel; B) average velocity in the channel (note that Treatments 2 and 3 plot nearly on top of each other); C) channel width median, 25th percentile, 75th percentile, maximum and minimum data not considered outliers, and outliers; and D) average wetted top width.

5. Discussion

The increased channel-floodplain connectivity observed in Treatment 1 is likely due to the low-lying inset floodplains, which were at least partially inundated at all modeled flows (pictured, planform in Fig. 5). The inundation of these features led to cross-meander flow contributing to high exchange rates between the channel and floodplain (Fig. 7). These well-connected inset floodplains also promoted flow thereby relieving maximum flows within the channel (Fig. 7B). The increased channel-floodplain connectivity of Treatment 1 was more pronounced during flows ≤6 m^3/s, but during the largest floods some metrics showed that Treatment 3 had similar channel-floodplain connectivity (Fig. 7). When comparing the regraded treatments, Treatment 3 had a higher floodplain volume and flow moving through the floodplain compared with Treatment 2 (Fig. 7A). This was probably due to the inset floodplain created in Treatment 3.

Floodplain and channel heterogeneities, including floodplain channels, create floodplain access at lower flows (Lewin et al. 2017; Czuba et al. 2019; Lindroth et al. 2020). Floodplain channels can be the first features of the floodplain to fill and relieve the main channel. This has been demonstrated using models of low gradient rivers that have high rates of exchange (Czuba et al. 2019). Restoration engineers may be able to incorporate more complex natural floodplain geometries, including floodplain channels to promote floodplain flow and relieve stresses in the main channel (McKean and Tonina 2013). Determining the sediment interactions in the floodplain is of particular concern for the study site because the stream reach is impaired for excess fine sediment loading. When designing and managing floodplains, the geometry and sediment load of the system must be considered as these factors impact whether the system is net erosional or depositional (Lewin et al. 2017; Sumaiya et al. 2021).

We believe that the high Treatment 1 channel floodplain connectivity is due to rapid channel adjustment that includes formation of the low-lying floodplain, but also results in increased bank erosion of opposite banks. More data are needed to determine the total volume of incoming and outgoing sediment, not just comparing

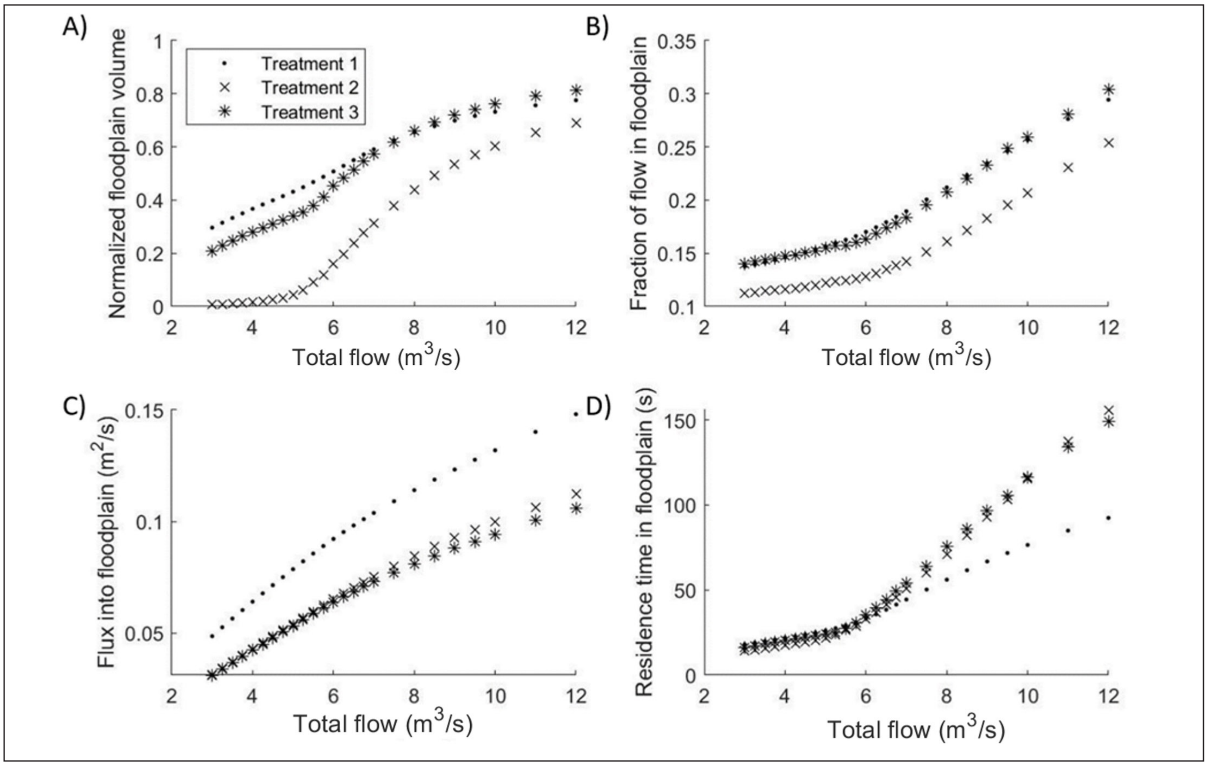

Fig. 7 Channel-floodplain connectivity metrics for each section including: A) normalized floodplain volume, B) fraction of discharge in the floodplain, C) volumetric flux into the floodplain per unit length of stream, and D) residence time in the floodplain.

pre- and post-cross sections. To determine the persistence of the high channel floodplain connectivity observed in Treatment 1, another survey in several years should be completed and this analysis should be repeated. The adjustments in Treatment 1 may be concerning as there is potential fine sediment load coming from the retreating banks, but it appears the floodplain building on the opposite bank offsets this, as Hendrix (2022) found that their monitored cross sectional-areas only in Treatments 1 and 2 are net depositional. However, a full sediment budget must be developed to determine if the channel adjustments have a significant impact on the overall sediment output of the system.

The high connectivity of Treatments 1 and 3 compared to Treatment 2 suggests that the stabilization without providing more connected features may have contributed to the lower channel-floodplain connection as defined in this study. This adverse impact of Treatment 2's stabilize-in-place method on channel-floodplain connectivity is described in recent theoretical frameworks of process-based restoration where arresting a degraded channel impedes evolution to more dynamically stable systems (Beechie et al. 2010; Castro and Thorne 2019). The creation of the inset floodplain in Treatment 3 offsets this impact providing higher volume and flow in its engineered inset floodplain, but regrading Treatment 3 did not produce the high exchange rate observed in Treatment 1.

While the results of this study showed that the treatment without regrading attained similar or higher channel-floodplain connectivity than the 2 common bank regrading techniques, we recognize that other factors can necessitate bank regrading and stabilization. Having relatively static reaches of streams is necessary in densely populated areas where migration could interfere with infrastructure or damage private property (Bernhardt et al. 2005). There must also be considerations for contaminated floodplain sediments, where leaving banks without stabilization has the potential to remobilize these pollutants (Gosar 2006; Kot et al. 2010). While the adjusted geometry of Treatment 1 provided floodplain access, this also led to reduced residence times in the floodplain. Though high channel-floodplain connectivity positively impacts nutrient attenuation (Clawson et al. 2001; Gergel et al. 2005; Shrestha et al. 2014; Regier et al. 2021), low residence times impede this function (Holmes et al. 1994; Zarnetske et al. 2011). Previous modeling of Treatments 2 and 3 suggested that widespread inset floodplains have the potential to increase geochemical cycling during floods but did not investigate the inset floodplain that has formed in Treatment 1 (Azinheira et al. 2014). Keeping these concerns in mind, application of passive techniques without bank stabilization can be used strategically where time and space for river adjustment and sediment mobilization are acceptable. In addition, while not included as part of this study, there are many other ecosystem services provided by stream restoration and riparian vegetation. The Treatment 2 sloped banks and Treatment 3 inset floodplains' riparian vegetation has grown extensively; large trees now partially or completely shade the stream channel (Resop et al. 2021) and woody debris is beginning to collect along the margins. Meanwhile, Treatment 1 has very few trees established, very little shading, and little to no woody debris build up: It is possible that the rapid channel evolution in this area makes it difficult for trees to establish along the inset floodplains.

In summary of the above discussion of results, we offer these key takeaways for future restoration work:

- High channel-floodplain connectivity may be achieved in an urban and agriculturally impacted system without regrading by allowing natural stream processes time and space for channel evolution.
- Where regrading treatments are implemented, an overemphasis on bank stability may impede channel-floodplain connectivity at the decadal scale.
- Heterogeneous floodplains with low-lying floodplain channels can form readily in channels that are allowed to evolve. In systems where stability is paramount, but channel-floodplain connectivity is desired, these features could be engineered through regrading.
- There is much more to stream restoration than just floodplain connectivity. The 2 main goals of the restoration project were "improve aquatic habitat" and "reduce sediment loading from eroding banks." We have ongoing research in place to evaluate these goals. In this paper and study, we are only assessing the changes in floodplain connectivity.
- More research is needed to assess overall sediment budgets of the 3 treatments (versus simple average cross-section change) in this complex, human-impacted, natural experiment.

Additional studies of floodplain connectivity should also investigate the unsteady flow attenuation of each treatment to better inform hydrologic models of peak flow attenuation in stream networks (Sholtes 2009; Dixon et al. 2016; Rajib et al. 2021; Knox et al. 2022). The higher connectivity of Treatment 1 suggests that it would attenuate peak flows more effectively than the other sections, but simulating unsteady flow hydrographs would shed light on this property more concretely. There is evidence that regraded streams can increase flood attenuation, but high roughness of a newly planted riparian buffer was deemed the main driver of this attenuation (McMillan and Noe 2017). Previous works do not include comparisons of peak flow attenuation in regraded streams with those where passive restoration techniques were implemented.

6. Conclusion

Channel-floodplain connectivity was examined in 3 different restoration treatments 11 years after restoration. Treatment 1 employed only cattle exclusion, Treatment 2 used bank stabilization on vertical or overhanging banks at a 3:1 slope, and Treatment 3 had the same stabilization treatment as Treatment 2 with the addition of an inset floodplain cut into previously vertical or overhanging banks. Treatment 2 produced the lowest channel-floodplain connectivity by almost all metrics. The high bank erosion rates in Treatment 1 are concerning for fine sediment loading, but an overall sediment budget needs to be completed to determine the fraction of sediment loading that comes from bank erosion and how much of this sediment builds new floodplain. The designed inset floodplain in Treatment 3 provided more floodplain volume and flow in the floodplain than Treatment 2 but failed to create the high channel-floodplain exchanges observed in the passive treatment as indicated by higher floodplain volume, channel-floodplain exchange flows, and flow moving across the floodplain. The self-formed floodplain configuration of Treatment 1 did not provide universally advantageous hydraulics. The floodplain width and residence time in Treatment 1 were lower than in Treatments 2 and 3. Despite the tradeoffs described above, this system serves as an example of how passive restoration techniques can create similar or higher channel-floodplain connectivity when compared with common regrading techniques. Practitioners may be able to mimic the features of the highly connected floodplain observed in this study by designing more heterogeneous floodplain surfaces with low-lying floodplain channels. Further, practitioners can learn that, for this system, stabilizing the banks reduced channel self-adjustment, potentially hampering the system's ability to regain high channel-floodplain connectivity.

Acknowledgements

This work was supported in part by the Virginia Agricultural Experiment Station (Blacksburg, Virginia, United States), the USDA National Institute of Food and Agriculture, and the U.S. Department of Agriculture Hatch program (1017457) (Washington, DC, United States). We would like to acknowledge support from the StREAM Lab manager and drone pilot, Laura Lehmann. We thank the production editor, Aimee Diehl, and co-editor in chief, Marc Beutel, for handling our manuscript, and the reviewers for their careful reading and valuable comments that improved the presentation of our work.

Author Contributions Statement

Conceptualization: NC; methodology: NC, JC, EMP, WCH; data analysis: NC, EMP; laboratory analyses: NC; EMP: writing original draft: NC; review/editing original draft: JC, EMP, WCH; investigation: NC, JC; resources: JC, WCH; data curation: NC, EMP, JC, WCH; supervision: JC, WCH; project administration: JC; funding acquisition: JC. All authors have read and agreed to the published version of the manuscript.

Conflict of Interest Statement

The authors have no conflict of interest to report.

Data Availability Statement

The DEM and lidar point cloud used in this model can be found at (Hession et al. 2023). All other elements necessary to recreate the final model, its outputs, and the scripts used to analyze these outputs are uploaded to Hydroshare and can be accessed at:

Christensen N. 2023. Christensen et al. JEED 2023 submission files, HydroShare, http://www.hydroshare.org/resource/843abe61dd8f4d668529740b27bf7cfe.

Related Publication Statement

This work was presented though Nicholas Christensen's Master's Thesis. It was also presented orally at the American Geophysical Union fall meeting 2022 by Nicholas Christensen.

Citations:

Christensen N. 2022. Comparison of hydraulic function and channel-floodplain connectivity between actively and passively restored reaches of Stroubles Creek 11 years after restoration [master's thesis]. Blacksburg (VA): Virginia Polytechnic Institute and State University. https://vtechworks.lib.vt.edu/handle/10919/110935.

Christensen N, Prior E, Czuba J, Hendrix C, Hession WC. 2022. Comparison of hydraulic function and channel-floodplain connectivity between actively and passively restored reaches of Stroubles Creek 11 years after restoration. Presentation at American Geophysical Union Fall Meeting; Chicago, US. Abstract available from: https://agu.confex.com/agu/fm22/meetingapp.cgi/Paper/1066689.

ORCID iDs

Nicholas D. Christensen
https://orcid.org/0009-0008-5309-7025
Elizabeth M. Prior
https://orcid.org/0000-0001-7069-160X
Jonathan A. Czuba
https://orcid.org/0000-0002-9485-2604
W. Cully Hession
https://orcid.org/0000-0002-6323-3827

References

Abel S, Hopkinson LC, Hession WC. 2016. Hydraulic and physical structure of runs and glides following stream restoration: structure of runs and glides following restoration. River Res Applic. 32(9):1890–1901. https://doi.org/10.1002/rra.3039.

Amoros C, Bornette G. 2002. Connectivity and biocomplexity in waterbodies of riverine floodplains: connectivity and biocomplexity in riverine floodplains. Freshwater Bio. 47(4):761–776. https://doi.org/10.1046/j.1365-2427.2002.00905.x.

Anderson W, Armstrong W, Armstrong R, Bailey P, Balch P, Barnes L, Beaver F, Bernard J, Beidenharn J, Bobowick D, et al. 2007. National engineering handbook part 654 stream restoration. Washington (DC): Natural Resource Conservation Service; [accessed 2023 Dec 29]. Available from: https://directives.sc.egov.usda.gov/OpenNonWebContent.aspx?content=17807.wba.

Azinheira DL, Scott DT, Hession W, Hester ET. 2014. Comparison of effects of inset floodplains and hyporheic exchange induced by in-stream structures on solute retention. Water Resour Res. 50(7):6168–6190. https://doi.org/10.1002/2013WR014400.

Baldwin D, Mitchell AM. 2000. The effects of drying and re-flooding on the sediment and soil nutrient dynamics of lowland river–floodplain systems: a synthesis. River Res Appl. 16:457–467. https://doi.org/10.1002/1099-1646(200009/10)16:5%3C457::AID-RRR597%3E3.0.CO;2-B.

Beechie TJ, Sear DA, Olden JD, Pess GR, Buffington JM, Moir H, Roni P, Pollock MM. 2010. Process-based principles for restoring river ecosystems. BioScience. 60(3):209–222. https://doi.org/10.1525/bio.2010.60.3.7.

Bellmore JR, Baxter CV. 2014. Effects of geomorphic process domains on river ecosystems: a comparison of floodplain and confined valley segments. River Res Appl. 30(5):617–630. https://doi.org/10.1002/rra.2672.

Bernhardt E, Palmer M. 2011. River Restoration: The fuzzy logic of repairing reaches to reverse catchment scale degradation. Ecol Appl. 21(6):1926–1931. https://doi.org/10.1890/10-1574.1.

Bernhardt E, Palmer MA, Allan JD, Alexander G, Barnas K, Brooks S, Carr J, Clayton S, Dahm C, Follstad-Shah J, et al. 2005. Synthesizing U.S. river restoration efforts. Science. 308(5722):636–637. https://doi.org/10.1126/science.1109769.

Brierley GJ, Fryirs KA. 2005. Geomorphology and river management: applications of the river styles framework. Malden, MA: Blackwell Pub. [accessed 2023 Oct 31]. https://doi.org/10.1002/9780470751367.

Brookes A, Shields FD, editors. 1996. River channel restoration: guiding principles for sustainable projects. Chichester; New York: J. Wiley.

Byrne CF, Stone MC, Morrison RR. 2019. Scalable flux metrics at the channel-floodplain interface as indicators of lateral surface connectivity during flood events. Water Resour Res. 55(11):9788–9807. https://doi.org/10.1029/2019WR026080.

Castro JM, Thorne CR. 2019. The stream evolution triangle: integrating geology, hydrology, and biology. River Res Applic. 35(4):315–326. https://doi.org/10.1002/rra.3421.

Chardon V, Schmitt L, Clutier A. 2022. Bank re-erosion action to promote sediment supply and channel diversification: feedback from a restoration test on the Rhine. River Res Applic. 38(5):975–987. https://doi.org/10.1002/rra.3968.

Clawson RG, Lockaby BG, Rummer B. 2001. Changes in production and nutrient cycling across a wetness gradient within a floodplain forest. Ecosystems. 4(2):126–138. https://doi.org/10.1007/s100210000063.

Czuba JA, David SR, Edmonds DA, Ward AS. 2019. Dynamics of surface-water connectivity in a low-gradient meandering river floodplain. Water Resour Res. 55(3):1849–1870. https://doi.org/10.1029/2018WR023527.

Dixon SJ, Sear DA, Odoni NA, Sykes T, Lane SN. 2016. The effects of river restoration on catchment scale flood risk and flood hydrology. Earth Surf Process Landforms. 41(7):997–1008. https://doi.org/10.1002/esp.3919.

Gergel SE, Carpenter SR, Stanley EH. 2005. Do dams and levees impact nitrogen cycling? Simulating the effects of flood alterations on floodplain denitrification. Global Change Biol. 11(8):1352–1367. https://doi.org/10.1111/j.1365-2486.2005.00966.x.

Gosar M. 2006. Mercury in river sediments, floodplains and plants growing thereon in the drainage area of the Idrija mine, Slovenia. Chin J Geochem. 25(S1):34–34. https://doi.org/10.1007/BF02839798.

Göthe E, Timmermann A, Januschke K, Baattrup-Pedersen A. 2016. Structural and functional responses of floodplain vegetation to stream ecosystem restoration. Hydrobiologia. 769(1):79–92. https://doi.org/10.1007/s10750-015-2401-3.

Hammersmark CT, Rains MC, Mount JF. 2008. Quantifying the hydrological effects of stream restoration in a montane meadow, northern California, USA. River Res Applic. 24(6):735–753. https://doi.org/10.1002/rra.1077.

Harman W, Starr R, Carter M, Tweedy K, Clemmons M, Suggs K, Miller C. 2012. A function-based framework for stream assessment and restoration projects. US Environmental Protection Agency, Office of Wetlands, Oceans, and Watersheds. Washington DC: EPA 843-K-12-006.

Hendrix C. 2022. Evaluating the Long-Term Morphological Response of a Headwater Stream to Three Restoration Technique. MS thesis. Blacksburg, VA: Virginia Tech, Department of Engineering. [accessed 2023 Oct 31]. http://hdl.handle.net/10919/111609.

Hession W, Lehmann L, Pingel T, Czuba J, Prior E, Christensen N, Kobayashi Y, Resop J. 2023. Virginia Tech StREAM Lab winter 2021 drone lidar survey. https://doi.org/10.5069/G9348HK3. [accessed 2023 Jun 7]. https://opentopography.org/dataspace/OTDS.042023.6346.1.

Holmes RM, Fisher SG, Grimm NB. 1994. Parafluvial nitrogen dynamics in a desert stream ecosystem. J North Am Benthol Soc. 13(4):468–478. https://doi.org/10.2307/1467844.

Karpack MN, Morrison RR, McManamay RA. 2020. Quantitative assessment of floodplain functionality using an index of integrity. Ecological Indicators. 111:106051. https://doi.org/10.1016/j.ecolind.2019.106051.

Knox RL, Morrison RR, Wohl EE. 2022. A river ran through it: floodplains as America's newest relict landform. Sci Adv. 8(25):eabo1082. https://doi.org/10.1126/sciadv.abo1082.

Kot FS, Bakanov KG, Goryachev NA. 2010. Mercury in bottom sediments of the Amur River, its flood-plain lakes and estuary, Eastern Siberia. Environ Monit Assess. 168(1–4):133–140. https://doi.org/10.1007/s10661-009-1097-0.

Lane SN. 2017. Natural flood management. WIREs Water. 4(3). https://doi.org/10.1002/wat2.1211.

Laub BG, McDonough OT, Needelman BA, Palmer MA. 2013. Comparison of designed channel restoration and riparian buffer restoration effects on riparian soils: stream restoration effects on riparian soils. Restor Ecol. 21(6):695–703. https://doi.org/10.1111/rec.12010.

Levell AP, Chang H. 2008. Monitoring the channel process of a stream restoration project in an urbanizing watershed: a case study of Kelley Creek, Oregon, USA: Urban Stream Restoration. River Res Applic. 24(2):169–182. https://doi.org/10.1002/rra.1050.

Lewin J, Ashworth PJ, Strick RJP. 2017. Spillage sedimentation on large river floodplains: spillage sedimentation on large river floodplains. Earth Surf Process Landforms. 42(2):290–305. https://doi.org/10.1002/esp.3996.

Lindroth EM, Rhoads BL, Castillo CR, Czuba JA, Güneralp İ, Edmonds D. 2020. Spatial variability in bankfull stage and bank elevations of lowland meandering rivers: relation to rating curves and channel planform characteristics. Water Resour Res. 56(8). https://doi.org/10.1029/2020WR027477.

McKean J, Tonina D. 2013. Bed stability in unconfined gravel bed mountain streams: with implications for salmon spawning viability in future climates: bed stability in unconfined streams. J Geophys Res Earth Surf. 118(3):1227–1240. https://doi.org/10.1002/jgrf.20092.

McMillan SK, Noe GB. 2017. Increasing floodplain connectivity through urban stream restoration increases nutrient and sediment retention. Ecological Engineering. 108:284–295. https://doi.org/10.1016/j.ecoleng.2017.08.006.

[OPUS] Online positioning user service. 2023. Washington D.C.: National Geodetic Survey [updated 2023 Dec 5; accessed 2023 Dec 22]. https://www.ngs.noaa.gov/OPUS/.

Opperman JJ, Luster R, McKenney BA, Roberts M, Meadows AW. 2010. Ecologically functional floodplains: connectivity, flow regime, and scale. JAWRA Journal of the American Water Resources Association. 46(2):211–226. https://doi.org/10.1111/j.1752-1688.2010.00426.x.

Palmer M, Ruhi A. 2019. Linkages between flow regime, biota, and ecosystem processes: implications for river restoration. Science. 365(6459):eaaw2087. https://doi.org/10.1126/science.aaw2087.

Pingel TJ, Clarke KC, McBride WA. 2013. An improved simple morphological filter for the terrain classification of airborne LIDAR data. ISPRS Journal of Photogrammetry and Remote Sensing. 77:21–30. https://doi.org/10.1016/j.isprsjprs.2012.12.002.

Prior EM, Aquilina CA, Czuba JA, Pingel TJ, Hession WC. 2021. Estimating floodplain vegetative roughness using drone-based laser scanning and structure from motion photogrammetry. Remote Sens. 13(13):2616. https://doi.org/10.3390/rs13132616.

Prior EM, Czuba JA, Pingel TJ, Thomas V, Randolph H, Wynne R, Hession WC. 2022. Investigating flood-vegetation interactions through remote sensing and modeling. Virginia Space Grant Consortium student research conference; 2022 April 22; Newport News (VA). https://vsgc.odu.edu/wp-content/uploads/2022/07/Prior.pdf.

Rajib A, Zheng Q, Golden H, Wu Q, Lane C, Christensen J, Morrison RR, Annis A, Nardi F. 2021. The changing face of floodplains in the Mississippi River Basin detected by a 60-year land use change dataset. Scientific Data. 8(27). https://doi.org/10.1038/s41597-021-01048-w.

Regier P, Ward ND, Indivero J, Wiese Moore C, Norwood M, Myers-Pigg A. 2021. Biogeochemical control points of connectivity between a tidal creek and its floodplain. Limnol Oceanogr Letters. 6(3):134–142. https://doi.org/10.1002/lol2.10183.

Resop JP, Hession WC, Wynn-Thompson T. 2014. Quantifying the parameter uncertainty in the cross-sectional dimensions for a stream restoration design of a gravel-bed stream. J Soil Water Conserv. 69 (4) 306-315. https://doi.org/10.2489/jswc.69.4.306.

Resop JP, Lehmann L, Hession WC. 2021. Quantifying the spatial variability of annual and seasonal changes in riverscape vegetation using drone laser scanning. Drones. 5(3):91. https://doi.org/10.3390/drones5030091.

Rubin Z, Kondolf G, Rios-Touma B. 2017. Evaluating Stream Restoration Projects: What Do We Learn from Monitoring? Water. 9(3):174. https://doi.org/10.3390/w9030174.

Sholtes J. 2009. Hydraulic analysis of stream restoration on flood wave propagation [master's thesis]. Chapel Hill (NC): University of North Carolina. https://doi.org/10.17615/s1ag-v630.

Shrestha J, Niklaus PA, Pasquale N, Huber B, Barnard RL, Frossard E, Schleppi P, Tockner K, Luster J. 2014. Flood pulses control soil nitrogen cycling in a dynamic river floodplain. Geoderma. 228–229:14–24. https://doi.org/10.1016/j.geoderma.2013.09.018.

Simon A, Bennett SJ, Castro JM. 2011. Stream restoration in dynamic fluvial systems: scientific approaches, analyses, and tools. Washington (DC): American Geophysical Union; [accessed 12/29/2023]. https://doi.org/10.1029/2011GM001099.

Simon A, Hupp C. 1987. Channel evolution in modified Tennessee channels. Transp Res Record. 1151. [accessed 2023 Oct 31]. https://onlinepubs.trb.org/Onlinepubs/trr/1987/1151/1151-002.pdf.

Sumaiya S, Czuba JA, Schubert JT, David SR, Johnston GH, Edmonds DA. 2021. Sediment Transport Potential in a Hydraulically Connected River and Floodplain-Channel System. Water Res. 57(5). https://doi.org/10.1029/2020WR028852.

Trimble SW. 1994. Erosional effects of cattle on streambanks in Tennessee, U.S.A. Earth Surf Process Landforms. 19(5):451–464. https://doi.org/10.1002/esp.3290190506.

[USEPA] U.S. Environmental Protection Agency. 2020. How's my waterway? 24060, Blacksburg, Virginia. Assessment Unit ID VAW-N22R_STE04A00. [accessed 2022 Oct 6]. https://mywaterway.epa.gov/waterbody-report/21VASWCB/VAW-N22R_STE04A00/2020.

[USGS 2019] U.S. Geological Survey. 2019. The StreamStats program. Washington (DC): U.S. Geological Survey; [accessed 2023 Dec 29]. https://streamstats.usgs.gov/ss/.

[USGS 2021] U.S. Geological Survey. 2021. 20210629, USGS 1 Meter 17 x54y412 VA_FEMA-NRCS_SouthCentral_2017_D17: U.S. Geological Survey. [accessed 2023 Oct 31]. https://www.sciencebase.gov/catalog/item/60ddf580d34e3a6dca28a0f7.

[Virginia FEMA] Virginia FEMA NRCS south central LiDAR B1. 2018. Washington D.C.: United States Geological Survey. [updated 2023 Aug 5; accessed 2023 Dec 22]. https://prd-tnm.s3.amazonaws.com/index.html?prefix=StagedProducts/Elevation/metadata/VA_FEMA-NRCS_SouthCentral_2017_D17/VA_South_Central_B1_2017/.

Wohl E, Lane SN, Wilcox AC. 2015. The science and practice of river restoration. Water Resour Res. 51(8):5974–5997. https://doi.org/10.1002/2014WR016874.

Wynn TM, Henderson MB, Vaughan DH. 2008. Changes in streambank erodibility and critical shear stress due to subaerial processes along a headwater stream, southwestern Virginia, USA. Geomorphology. 97(3–4):260–273. https://doi.org/10.1016/j.geomorph.2007.08.010.

Wynn-Thompson T, Hession WC, Yagow G. 2010. Final Project Report Stroubles Creek Stream Restoration. Richmond VA; Virginia Department of Conservation and Recreation. https://vtstreamlab.weebly.com/uploads/4/3/7/4/43749251/stroubles_restoration_wqif_final_report.pdf.

Zarnetske JP, Haggerty R, Wondzell SM, Baker MA. 2011. Dynamics of nitrate production and removal as a function of residence time in the hyporheic zone. J Geophys Res. 116(G1):G01025. https://doi.org/10.1029/2010JG001356.